Current Medical Imaging Reviews, 2005, *1*, 229-243

Current Issues in the Utility of Blood Oxygen Level Dependent MRI for the Assessment of Modulations in Tumor Oxygenation

Christine Baudelet and Bernard Gallez*

Laboratory of Biomedical Magnetic Resonance and Medicinal Chemistry Unit, Université Catholique de Louvain, Brussels, Belgium

Abstract: It has been known for some time now that hypoxia is an important physiological parameter in tumor growth and response to therapy. The development and application of non invasive methods to determine the extent of tumor hypoxia as well as its modulation will improve cancer treatment strategies. Magnetic Resonance sequences that are based on the BOLD effect use the endogenous contrast agent deoxyhemoglobin as a source of contrast. This technique can be used to monitor the evolution of tumor oxygenation since there is a good correlation between the evolution of the partial pressure of oxygen (pO_2) and the NMR parameters measured. The information provided by BOLD NMR is essentially qualitative in nature due to the complexity of the relationship between the pO_2 and the NMR parameters measured. The factors at the origin of this complex relationship are discussed in this review. The advantages of the BOLD technique are non invasiveness and high spatial and temporal resolution. The method has been successfully applied in experimental and human tumors to monitor changes after respiratory challenges and pharmacological treatments. Additionally, the method has been used to provide maps of mature and functional tumor vessels and maps of spontaneous fluctuations of oxygenation and blood perfusion related to tumor acute hypoxia.

Keywords: Tumor hypoxia, pO_2, BOLD MRI, susceptibility, angiogenesis, blood flow.

INTRODUCTION

Blood flow and oxygenation are crucial factors in cancer therapy. In order to improve clinical outcomes, efforts must be made to understand further the mechanisms underlying hypoxia and to develop ways to modulate and assess hypoxia. The blood oxygen level dependent (BOLD) MRI imaging technique has the unique capability to study tumor pathophysiology non-invasively. In this article, the importance of tumor hypoxia will first be briefly reviewed. Then, a summary of the use of BOLD MRI to study tumor oxygenation and tumor development will be provided.

CAUSES OF TUMOR HYPOXIA

It has been known for a long time that hypoxia is an important physiological parameter in tumor growth and response to therapy [1]. Mechanistically, tumor hypoxia results from an imbalance between oxygen delivery and oxygen consumption. On the one hand, the oxygen delivery is impaired by structural abnormalities present in the tumor vasculature [2]. Tumor vasculature frequently has disorganized vascular networks, dilatation, elongated and tortuous shapes, incomplete endothelial linings, and defective basement membranes. These structural abnormalities cause numerous functional impairments, such as increased transcapillary permeability, interstitial hypertension, and increased flow resistance, thereby compromising O_2 supply [3,4]. On the other hand, the altered tumor cell metabolism with elevated metabolic rates also contributes to the occurrence of hypoxic regions in tumors [5]. It is generally believed that tumor hypoxia develops in two ways: chronic hypoxia (or diffusion-limited hypoxia) and acute hypoxia (or perfusion-limited or fluctuating hypoxia) [6]. Diffusion-limited (chronic) hypoxia is caused by an increase in diffusion distance between tumor vessels with tumor expansion [7]. This results in an inadequate O_2 supply for cells distant (>70μm) from nutritive blood vessels. Steep longitudinal gradients of pO_2 along the vascular tree, as opposed to radial diffusion of oxygen, can also contribute to deficiencies in tumor oxygen supply [8]. Another important feature is the irregular geometry of vascular networks. Secomb *et al.* [9] developed a scenario where there is adequate vascular density, but the chaotic nature of the vascular geometry creates hypoxia. Abnormal branching angles lead to situations where vessels carry plasma but no red blood cells.

Acute (perfusion related) hypoxia is caused by blood flow instabilities and vascular stasis, resulting from the severe structural and functional abnormalities in tumor microvasculature. Factors that may contribute to flow fluctuations include arteriolar vasomotion [10,11], rapid vascular modeling [12], and other hemodynamic effects such as non linear flow properties of blood, nonuniform axial distribution of red blood cells within the vessel, or disproportionate cell partitioning at bifurcations [13]. In addition, it has been demonstrated theoretically that in the presence of moderate leakiness, the fluid dynamics of tumor circulation evolves toward a sustained oscillatory response, both in the microvascular pressure and blood flow [14].

CONSEQUENCES OF TUMOR HYPOXIA

Experimental and clinical evidence suggest that the hypoxic fraction in solid tumors may: 1) promote metastasis, 2) select cells with a malignant phenotype, 3) promote

*Address correspondence to this author at the CMFA / REMA units, Université Catholique de Louvain, E. Mounier Avenue, 73.40; B-1200 Brussels, Belgium ; Tel/Fax: 32 2 764 2790; E-mail: gallez@cmfa.ucl.ac.be

1573-4056/05 $50.00+.00

angiogenesis, and 4) increase resistance to radiation therapy and other cancer treatments.

Tumor Hypoxia Promotes Metastasis

Several experimental models have shown that tumor hypoxia is associated with an increased ability to form metastases [15]. Young and co-workers demonstrated many years ago that murine tumor cells exposed to severe hypoxia increased their metastatic potential [16]. The causal link between hypoxia and metastasis was later demonstrated *in vivo*. Hypoxia is able to promote tumor metastasis in two ways: 1) by inducing the expression of gene products involved in the metastatic cascade and 2) by providing selection pressure for a more aggressive phenotype. The initiation of metastasis is a multiple pathway that involves three major processes: degradation of the basement membrane and extracellular matrix, modulation of cell adhesion molecules, and cell migration. The effects of low pO_2 on metastasis are correlated to expression of vascular endothelial growth factor (VEGF) [17]. Low pO_2 increases metastasis whether the cells are treated *in vitro* prior to injection [16] or the whole animal is exposed to transient hypoxia [18].

Tumor Hypoxia Selects Cells with a More Malignant Phenotype

Hypoxia provides a physiological selective pressure in tumors for the expansion of variants that have lost their apoptotic potential, and in particular for cells acquiring p53 mutations [19]. The selective pressure resulting from hypoxia is not limited to the selection of cells with reduced apoptotic potential. It has also been shown to provide a possible selection force for cells that have altered oncogenic pathways that result in a switch to a more angiogenic phenotype. By promoting the clonal expansion of cells with reduced apoptosis and increased angiogenesis, hypoxia can contribute to the development and malignancy of tumors. Clinical results showing that hypoxic cervical cancers with low apoptotic index are highly aggressive support this basic experimental concept [20].

Tumor Hypoxia Promotes Angiogenesis

Tumor progression requires the formation of new blood vessels in order to provide nutrients and remove catabolites from the expanding tumor mass. Angiogenesis is also essential for the efficient dissemination of primary tumor cells during metastasis. The early steps of angiogenesis in tumors are nearly identical, as both processes involve degradation of the extracellular matrix and directed migration of either vascular or neoplastic cells. In addition, angiogenesis requires proliferation of the migrating endothelial cells. Initiation of angiogenesis begins when cells within the tumor microenvironment respond to hypoxia by the production of VEGF. In addition to VEGF, hypoxia is also responsible for inducing the expression of the VEGF receptors (VEGFR1 and VEGFR2) through HIF-1 mediated transcription [21].

Changes in Gene Expression that Accompany Tumor Hypoxia

The multiple roles assigned to hypoxia, including the induction of angiogenesis, apoptosis and metastasis, likely result in large part from changes in gene expression that accompany hypoxia [22]. A significant number and wide variety of hypoxia-induced genes have been described including oncogenes, tumor-suppressor genes, stress proteins, and cytokines. Cells exposed to hypoxia upregulate the expression of several transcription factors. Perhaps the most important within this group is HIF-1, which induces the expression of more than 60 known genes, essential for glucose metabolism (e.g. glucose transporters GLUT-1 and GLUT-3), for iron metabolism (e.g. transferrin and its receptor), for hormones regulation (e.g. erythropoietin), and for vasoreactivity (e.g. endothelin-1, nitric oxide synthase, VEGF) [23].

Tumor Hypoxia Increases the Resistance to Radiotherapy

Tumor hypoxia causes severe problems for radiation therapy (X and γ radiation), because the radiosensitivity is progressively limited when the pO_2 is below 10 mm Hg [24,25]. Hypoxia-associated resistance to photon radiotherapy is multifactorial. The presence of molecular oxygen increases DNA damage through the formation of oxygen free radicals, which occurs primarily after the interaction of radiation with intracellular water. Because of this so-called "oxygen enhancement effect", the radiation dose required to achieve the same biologic effect is about three times higher in the absence of oxygen than in the presence of normal levels of oxygen. The critical value is about 5 mm Hg. In a series of experimental and clinical studies, Vaupel and others showed definitively that measurements of pO_2 by polarographic microelectrodes provided useful criteria for predicting the response of tumors to radiation therapy [26-30]. Also, magnetic resonance studies showed similar data relating tumor response to irradiation with respect to estimated initial pO_2 value [31-33].

Tumor Hypoxia Diminishes Chemotherapeutic Efficacy

Tumor hypoxia has been shown to decrease the efficacy of cytotoxic drugs [34]. Cells located distant from a functional blood supply can be resistant to drug therapy because of several factors. First, a limited penetration of anti-cancer agents would result in lower efficacy. It has indeed been shown that the drug toxicity falls off as a function of distance from blood vessels [35]. Second, as a result of decline in nutrient and oxygen availability, cells further away from the vascular system would be dividing at a reduced rate and thus would be protected from the effects of chemotherapeutic agents whose activity is selective for rapidly dividing cell populations. Besides the inhibition of cell proliferation, multiple mechanisms are probably also involved in the hypoxia-induced resistance to chemotherapeutic agents, for example hypoxia-induced decreased cytotoxicity of certain agents, and tissue acidosis. Furthermore, hypoxic stress proteins and the loss of apoptotic potential can impart resistance to certain chemotherapeutic drugs. Paradoxically, hypoxic cells can be exploited for therapy by non-toxic, hypoxia-activated prodrugs. Also, bioreductive drugs are preferentially toxic to tumor cells in a hypoxic environment (e.g. tirapazamine) [36]. Finally, the resistance of solid tumors to chemotherapy may also be the result of another largely ignored factor: tumor specific fluctuations in blood flow. Fluctuating

hypoxia has significant implications for delivery of chemotherapeutic agents, cellular responsiveness to those agents, and the regrowth potential of the surviving tumor cells [37]. Moreover, regions actively proliferating at one point in time may not have cells actively synthesising DNA at a different time.

BOLD MRI

The assessment of tumor oxygenation may have profound therapeutic implications in oncology. Hence, a non-invasive technique that could accurately and repetitively measure tumor oxygenation would find broad applications in clinical and basic research. Different imaging modalities are currently under development to provide oxygen mapping. These include near-infrared imaging [38], nuclear medicine techniques (PET, SPECT) [39,40], electron paramagnetic resonance imaging / spectroscopy [41], dynamic nuclear polarization [42], and ^{19}F-NMR techniques [43,44] and BOLD-based MRI [45]. In the present article, we will focus on BOLD-dependent MR imaging methods.

BOLD CONTRAST: THEORETICAL AND TECHNICAL CONSIDERATIONS

BOLD MR imaging—the blood oxygen level-dependent (BOLD) contrast mechanism in brain was first described by Ogawa *et al.* in rat studies using NMR at strong magnetic fields (7 and 8.4 T) [46]. Ogawa noticed that the contrast of very high resolution images acquired with a gradient-echo pulse sequence depicts anatomical details of the brain as numerous dark lines of varying thickness. By accentuating the susceptibility effect of deoxyhemoglobin (dHb) in the venous blood with gradient-echo techniques, they discovered that image contrast reflected the blood oxygen level. As it is now known, the phenomenon is indeed due to the field inhomogeneities induced by the endogenous MRI contrast agent dHb. In dHb, the iron (Fe^{2+}) is in a paramagnetic high spin state (d4), as four out of six outer electrons are unpaired. The paramagnetic nature of dHb can modify the strength of the magnetic field passing through it. It enhances the R_2 (=1/T_2) and R_2* (=1/T_2*) transverse relaxation rates of water in blood and in the tissue surrounding the blood vessels [47]. [Of note, T_2 and T_2* are time constants that characterize the rate at which the transverse magnetization decays. Unlike T_2, T_2* is sensitive to inhomogeneities in the magnetic field with the result of rapid loss in transverse magnetization and MRI signal]. Changes in R_2 reflect the capillary microvasculature whereas R_2* is sensitive to both micro- and macrovasculature [48]. In the simplest model, these relaxation rates change linearly with deoxyhemoglobin concentration, which therefore acts as an endogenous contrast agent for blood oxygenation. Equation [1] shows the linear relationship between ΔR_2* and content of deoxyhemoglobin. Some studies have also reported a quadratic function between blood R_2* and oxygen saturation, suggesting that the technique should be more sensitive in regions with low oxygen saturation, e.g. in tumors [49,50].

$$R^*_2 = R^*_{20}tissue + k[dHb], \qquad [1]$$

where k depends on field strength, blood vessel orientation and morphology, [dHb] is the tissue deoxyhemoglobin concentration. R_2*$_0$ tissue is the intrinsic transverse relaxation rate of the tissue and is assumed to be a static component. It includes R_2, the relaxation rate of the tissue and magnetic field inhomogeneity due to susceptibility variations determined by the tissue structure and content, excluding erythrocytes.

Gradient echo images are usually employed for BOLD imaging. On T_2* weighted images, the signal intensity (SI) from a gradient recalled echo sequence is given by:

$$SI = S_0 \sin(a)\, exp(-TE/T2^*), \qquad [2]$$

where S_0 is proportional to the proton density, α is the flip angle, and TE is the echo time.

A change in R_2* (ΔR_2^*) can be calculated from T_2* weighted signal changes as:

$$\Delta R^*_2 = \frac{1}{TE} \ln\left(\frac{SI_{pre}}{SI_{post}}\right), \qquad [3]$$

where TE is the echo time and SI is the signal intensity from T_2* weighted images.

Both ΔR_2^* and relative change in signal intensity (%ΔSI= SI_{post}/SI_{pre}) are parameters that are proportional to the change in deoxyhemoglobin content, independent of native tissue $R_2^*{}_0$. On the contrary, absolute change in signal intensity (ΔSI= SI_{post}- SI_{pre}), and ΔT_2* are parameters that are sensitive to the native tissue $R_2^*{}_0$. The consequence of this is that [dHb] changes cannot be reliably inferred from ΔT_2* or ΔSI when different tissue regions are compared. For example, regions with high signal intensity in T_2*w GRE images (high T_2* tissue) will display more signal change in response to the same change in [dHb] than regions with low SI (low T_2* tissue) and similar basal content in dHb (see Fig. **1**).

The relations described here above are further complicated by the fact that at short repetition time (TR) and high flip angle (30-90°), GRE images are also sensitive to flow. The water in blood flowing into the imaging slice produces a much stronger signal than that from water in static tissue, because the spins in the static tissue will have been partially saturated by previous radiofrequency pulses (see Fig. **2**). When there is an increase in blood flow, there is signal enhancement that is generally known as the "in-flow effect" [51]. To emphasize the importance of flow effects, the term FLOOD (flow and oxygenation dependent contrast) MRI has been used [52].

The steady state signal intensity from a gradient recalled echo sequence is given more generally by:

$$S = S_0 \sin(\alpha) \exp(-TE/T_2^*) \frac{(1-\exp(-TR/T_1)}{1-\cos(\alpha).\exp(-TR/T_1)}, \qquad [4]$$

where S_0 is proportional to the proton density, α is the flip angle, TE is the echo time and TR is the repetition time. T_1 is the apparent longitudinal relaxation time and takes into account "in-flow" effects that are significant at short TR.

To distinguish the contribution from the inflow and blood oxygenation to the BOLD signals, multiple gradient-echo imaging sequences (extraction of R_2^* values) is used instead

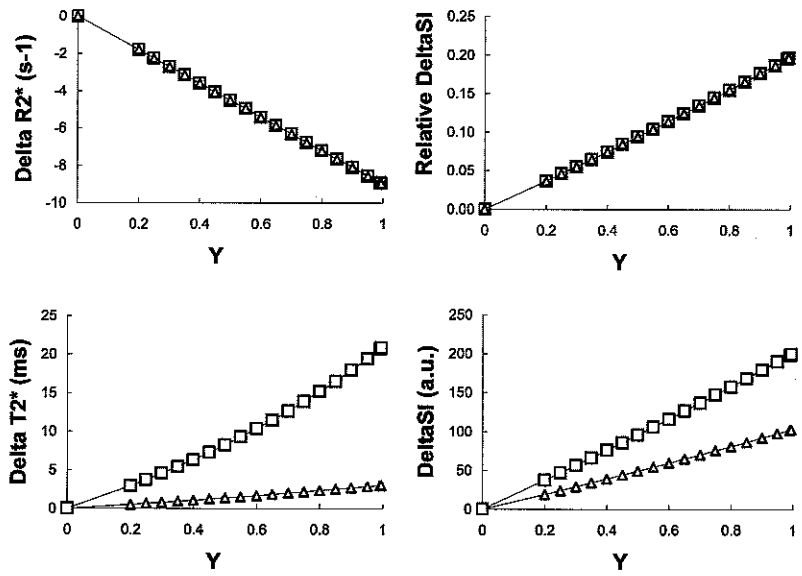

Fig. (1). Theoretical simulation of changes in tumor R_2*, T_2*(=1/R_2*), %SI and SI as a function of O_2-hemoglobin saturation (Y=1: fully saturated), modulating deoxyhemoglobin content. Effect of intrinsic T_2*$_0$ tissue: 20ms (Δ), and 60ms ( ). Fixed parameters used are: hematocrit fraction: 0.45, blood volume fraction: 0.05, proportionality constant k: 400 s-1, flip angle: 45°, TR: 200ms, TE: 20ms, and S_0: 2000.

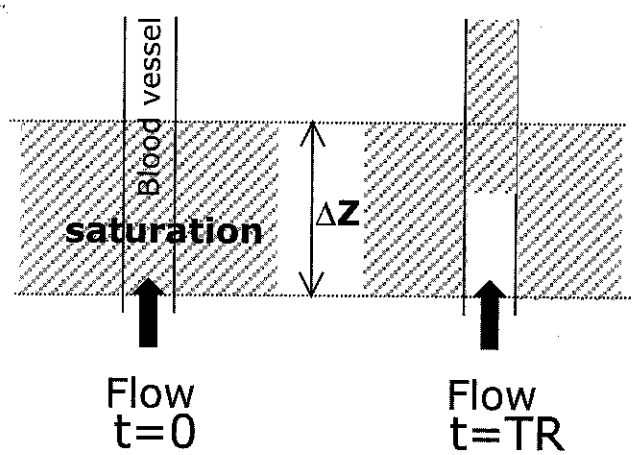

Fig. (2). Inflow effect, when fully magnetized spins are swept into an imaged section (ΔZ) from the outside by flow. This effect is significant when the average flow velocity is sufficiently large that a substantial fraction of the spins in the imaged section is replaced during the repetition time TR of the pulse sequence.

of using conventional gradient-echo techniques [53]. Inflow effects can be also eliminated by using low flip angle, centrically ordered k-space trajectories or inter-image delays. The effectiveness of the flow suppression technique is based on the fact that tissue longitudinal magnetization is allowed to recover nearly completely prior to each collection of the center of k-space. With no magnetization saturation, there can be no in-flow enhancement.

BOLD contrast changes can also be detected with high spectral and spatial resolution (HiSS) MRI rather than with GRE imaging [54-56]. Most MRI methods assume that the water resonance behaves as a single Lorentzian distribution of frequencies. However, HiSS imaging has shown that in some voxels the water resonance is complex, with many resolvable frequency components. The origin of these frequency shifts is not known, but they likely represent a subvoxel distribution of water in distinct magnetic environments. This effect is especially strong in and near tumors, where deoxygenated blood and a generally heterogeneous environment produce broad, complicated water lines. The detailed structure of the water line can be an important source of information regarding local (subpixel) anatomy and physiology and can be analyzed to improve contrast and accuracy on HiSS MR images. HiSS is a natural extension of the work of previous investigators, beginning with Dixon [57] and Glover [58], who used low-resolution spectroscopic imaging to separate fat and water and correct distortions due to B0 inhomogeneity. More recently, advances in MR hardware and software have allowed rapid acquisition of echo-planar spectroscopic imaging (EPSI), at very high spectral and spatial resolution. As a result, the details of the water and fat line shapes in each very small image pixel can be resolved with reasonable acquisition times [59]. HiSS datasets can be used to synthesize images in which intensity is proportional to peak height, peak frequency, or linewidth. Changes in the water signal linewidth, which are proportional to changes in R_2*, has been reported to detect BOLD contrast change in tumors during carbogen breathing [55,56]. HiSS MRI can emphasize changes in necrotic and/or hemorrhagic regions, so that it is more sensitive to oxygenation changes compared to conventional MRI.

PARAMETERS AFFECTING THE BOLD CONTRAST IN TUMORS

The use of BOLD contrast in tumors is a new area of research and brings with it new challenges of understanding

Table 1. Comparison of Brain and Tumor Characteristics in Relation to BOLD Imaging

Brain	Tumor
▪ Blood flow regulated	▪ Poor blood flow regulation leading to hypoxia
▪ Oxidative metabolism	▪ Mixed glycolytic and oxidative metabolism
▪ Uniform capillary and tissue density	▪ Heterogeneous capillary and cell density
▪ Well structured vascular architecture and capillary network	▪ Chaotic architecture of structurally and functionally abnormal blood vessels

and interpretation. The underlying physiological changes are different from those of BOLD in the brain. In the brain, blood vessel size, density and distribution are well characterized, contrary to tumors (see Table 1). The assumptions used in models to describe BOLD contrast of fMRI in brain cannot therefore be applied.

Generally, a change in tumor R_2* can result from changes in blood oxygen saturation, hematocrit, or blood volume, given that all of these parameters determine the deoxyhemoglobin content [52].

$$R^*_2 = R^*_{20}\,tissue + ki\,[Hct_i\,Bv_i\,(1 - Y_i)] \qquad [5]$$

where BV_i is the blood volume, Y_i the blood hemoglobin saturation, Hct_i is the fractional hematocrit and k_i depends on field strength, blood vessel orientation and morphology. The subscript i correspond to arterioles (a), capillaries (c) and venules (v), and within a single voxel, the total contribution to R_2* relaxation of blood theoretically is a linear sum of the individual rates [46].

From this equation, it can be observed that blood oxygenation and blood volume are competing parameters with opposite effect on R_2*. A vasoactive challenge that improves blood flow and so decreases the blood desaturation (assuming that no change in metabolic rate occurs) is likely to be associated with a blood volume increase. Whether this produces a decrease in R_2* depends on the balance between changes in flow and volume with any change in oxygenation utilization, and this balance is generally unknown for tumors [52]. Another possible confounding factor in correlating the change in R_2* due to changes in blood oxygen saturation with tissue oxygenation is a change in blood pH. Acidification (e.g. during carbogen breathing) can be responsible for a right shift of the oxygen saturation curve due to the Bohr effect [60], and so results in fractional increase in deoxyhemoglobin and consequently in an increase in R_2*. Metabolic changes associated with vasoactive challenges also have an unpredictable influence on blood saturation and R_2*. Acute hyperglycemia, for example, may transiently reduce the oxygen consumption rate of tumor cells by inducing a metabolic shift from cell respiration to glycolysis (Crabtree effect) [61]. Conversely, the additional glucose may stimulate oxidative metabolism [62].

It can also be inferred from equation [5] that the size of R_2* change upon a given change in blood oxygenation is modulated by the blood volume, i.e. tumors with highly vascularized regions would most likely show the greatest change in R_2*.

CORRELATION BETWEEN BOLD MRI AND TUMOR PO_2

How do Changes in BOLD Parameters Parallel Changes in pO_2 in Tumors?

BOLD MRI, because of its sensitivity to blood oxygenation, may provide a measure of tumor oxygen tension (oxygen in the extravascular space). Since this parameter is highly relevant for treatment outcome (e.g. it determines the radiosensitivity of the tumor), there is a need to know how R_2* or T_2*-weighted signal and tumor pO_2 are quantitatively correlated. Several studies have investigated the correlation between the amplitude of the BOLD response in tumor upon hyperoxic gas breathing and corresponding changes in tumor pO_2. Robinson *et al.* investigated the relationship between GRE MRI response during carbogen breathing and tumor pO_2 changes using invasive Eppendorf histography [63]. An apparent lack of correlation between BOLD MRI and pO_2 histography was observed. By contrast, Al Hallaq *et al.* observed a strong correlation between water resonance linewidth decrease and O_2 microelectrode data during carbogen breathing, averaged over the whole tumor [64]. Maxwell *et al.* performed simultaneous measurement of BOLD signal and pO_2 using an MR-compatible fiber-optic oxygen sensor during carbogen breathing. They observed a good temporal correlation between the increase in GRE signal intensity averaged over the whole tumor and the increase in oxygenation status. We also evaluated the correlation between BOLD MRI signal intensity or R_2* and tumor pO_2 using fiber-optic microprobes implanted in the tumor [49]. We found that the evolution of the *local* BOLD response (SI or T_2*) was temporally positively correlated with the local corresponding change in pO_2 (see Fig. **3**) However, we also demonstrated that BOLD MRI does not provide a quantitative measurement of the evolution of pO_2. For example, we observed a more pronounced increase in signal intensity (or decrease in R_2*) when passing from 5 to 15 mmHg than when passing from 40 to 50 mmHg (see Fig. **4**). Because of the curvilinear relationship and a lack of baseline pO_2 estimation, a variation of R_2* or signal intensity could not be related quantitatively to the response in pO_2.

Maxwell RJ, Robinson SP, Mc Intyre DJO, *et al.* Simultaneous measurement of gradient-echo 1H MR images and pO2 using a fiber-optic oxygen sensor in rodent tumours and their response to carbogen breathing. 6th Annual Meeting of the International Society for Magnetic Resonance in Medicine 1998; 1665.

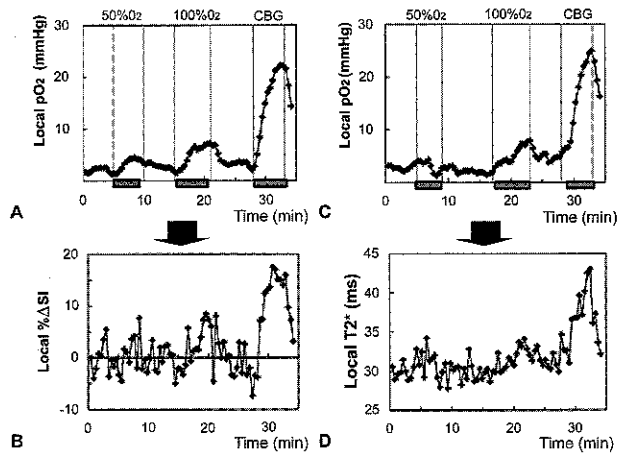

Fig. (3). Time courses of relative change in T_2*w GRE signal intensity (B) and T_2* (D) during respiratory challenges (air-50%O_2-air-100%O_2-air-carbogen-air) in a FSa tumor and corresponding local changes in tumor pO_2 (A, C), as measured concomitantly by a fiber-optic microprobe. *Adapted from ref [49].*

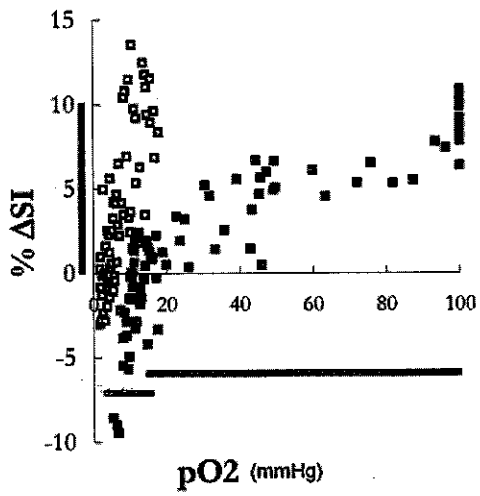

Fig. (4). Relative changes in T_2*w GRE signal intensity as a function of tumor pO2 as modulated by the use hyperoxic gas breathing. A 10 percent change in SI can reflect a variation of less than 20 mmHg in one tumor (□) but about 80 mmHg in another one (■). *Adapted from ref [49].*

Moreover, the sensitivity of R_2* to the change in pO_2 was variable from one tumor to another, suggesting that any comparison of responses between different tumors or different locations within the same tumor should be made with caution. The blood volume fraction may vary within a tumor (and necessarily between tumors) and thereby influences BOLD sensitivity (see eqn 5).

Fan *et al.* performed a comparison between BOLD MRI measurements and quantitative ^{19}F imaging of tumor pO_2.[54]. The ^{19}F spin-lattice relaxation rate R_1 was measured to determine pO_2 in each image pixel containing perfluorocarbon (PFC), and changes in pO_2 during carbogen breathing. These parameters could be correlated on a pixel-by-pixel basis with changes in water signal linewidth (which are proportional to change in R_2*). In hypoxic regions, ^{19}F and ^1H MRI both showed that carbogen had relatively weak effects. However, BOLD MRI sometimes failed to detect significant increases in pO_2 that were reported by ^{19}F MRI. According to the authors, this lack of sensitivity could be explained by several factors. First, limited spectral/spatial resolution could have been insufficient to detect small changes in R_2*. Second, BOLD MRI is probably less sensitive to changes in tumor oxygenation in regions containing very sparse vasculature and thus small amounts of deoxyhemoglobin (see eqn.5). Third, deoxyhemoglobin changes in large vessels may dominate BOLD contrast, which may not well be correlated with tissue pO_2. This problem should be avoided in spin echo images which are more sensitive to BOLD contrast in smaller vessels where intra and extravascular pO_2 are more tightly coupled [65]. Furthermore, quantitative changes in ^{19}F R_1 vs. ^1H T_2* were poorly correlated, reflecting the fact that changes in BOLD contrast in tumors do not provide a quantitative measure of changes in pO_2. However, when results for the entire tumor are averaged together, the correlation improves. This suggests that spatial resolution of the measurements can greatly affect agreement between both techniques. Indeed, when changes are averaged over the whole tumor, the regional heterogeneity of vascular volume distribution or changes in blood oxygen is smoothed out. Thus, a better correlation between BOLD contrast and pO_2 might be observed when the tumor is studied globally.

BOLD MRI has also been correlated with the EPR oximetry technique. Localized absolute measurements of pO_2 using EPR oximetry indicated that carbogen breathing increased tumor oxygenation, thereby corroborating BOLD contrast results [66,67]. Williams *et al.* have compared BOLD MRI with electron paramagnetic resonance imaging (EPRI), a promising new imaging modality capable of providing quantitative, relatively high-resolution maps of the concentration of oxygen in the tissue fluids of living animals. Images were obtained from a tumor bearing mice during a carbogen breathing challenge. A good spatial correlation was

found between EPRI spin probe distribution and areas of the tumor demonstrating BOLD signal changes [68]. Well-vascularized tumor portions, contrary to necrotic regions, allowed the distribution of the spin probe via the vasculature and responded to a change in the fraction of inhaled oxygen. Elas *et al.* investigated the correlation between oxygen images obtained with EPRI and BOLD MRI [69]. There appeared to be a good correlation between the regional variation in the BOLD and EPR images.

The capacity of BOLD MRI to monitor changes in tumor oxygenation during carbogen breathing is thus well established. The qualitative nature of the technique has been put forward, with vascular fraction or baseline pO_2 being crucial parameters determining the sensitivity of the BOLD contrast. The effects of other vasomodulators on tumor oxygenation have been studied using the BOLD MRI technique. We will discuss it later on.

Basal R_2* as a Method to Evaluate Tumor Hypoxia?

The potential use of basal R_2* as an estimator of tumor oxygenation has also been evaluated. This could provide a non-invasive method to measure the oxygenation status of tumors. Methods for rapidly assessing hypoxia in an individual tumor would clearly improve cancer treatment strategies. Tumor basal R_2* may potentially be considered as an intrinsic marker of pO_2, since it is related to the oxygenation state of hemoglobin and to the arterial blood pO_2 which is in equilibrium with tissue pO_2. The baseline R_2* contains a component that depends on the tumor tissue deoxyhemoglobin content, which is a function of the vascular volume of the tumor (see eqn 5). Assuming that this vascular volume is actively perfused by erythrocytes, the R_2* may be viewed as a potential estimator of tumor oxygenation (elevated R_2* in case of low oxygen tension). A mapping of R_2* would display the heterogeneity of pO_2 inside the tumor. We investigated the correlation between basal R_2* and pO_2 using co-registered and simultaneous measurement [49]. A poor correlation was found between both parameters, suggesting that measuring R_2* is not a relevant method to evaluate tumor oxygenation. The theory concerning R_2* predicts this result. R_2* is the result of the inherent relaxation time (R_2) and an additional dephasing component (R_2') arising from magnetic field inhomogeneities which increase R_2*. Dephasing effects include: i) magnet imperfections, ii) magnetic susceptibility variations within the sample, such as air-tissue interfaces or local hemorrhage. All these parameters affect R_2* independent of any physiological process associated with BOLD contrast. Consequently, estimation of the relative contribution of the physiological process to the R_2* value is not trivial. An extreme example is the case of head and neck tumors, where parts of tumors are completely obscured by susceptibility artefacts near air cavities [70]. It is clear in this case that R_2* (high values, rapid dephasing) is not correlated to tumor pO_2. Common approaches to compensate these unwanted local susceptibility gradients in the slice selection direction are z-shimming [71] or the use of tailored radio frequency pulses [72]. Whether such methods can improve the correlation between native R_2* and pO_2 remains to be evaluated. Additionally, necrotic areas are often hyperintense on T_2* weighted images (low R_2* value) and yet of course pO_2 values are nearly zero.

Additionally, from equation 5 it is clear that R_2* is not simply determined by the intravascular oxygenation status but rather by the dHb content inside the image element. At similar vessel oxygenation, higher vascular density will lead to higher R_2*, and yet this would not result in lower tissular oxygenation. Hence, when comparing tumors with different vascular densities, a positive correlation between R2* and tumor oxygen tension can be observed, instead of negative one. Some recent studies have revealed that high values for R_2* could reflect how well the tumor is vascularized. Also, intrinsic susceptibility magnetic resonance imaging can be used as a complementary approach to assess tumor angiogenesis (see next section). Rodrigues *et al.* showed that tumor R_2* could provide prognostic indicators of acute radiotherapeutic response [73]. They used two rodent tumor models which exhibited very different baseline values of R_2*. GH3 prolactinomas, which exhibited faster baseline R_2* (and also greater carbogen-induced ΔR_2*), appeared to be more responsive to radiotherapy than RIF-1 fibrosacrcomas with lower baseline R_2*. GH3 prolactinomas, tumors with faster baseline R_2*, had greater blood volume, perfused vascular fraction and microvessel size than RIF-1 fibrosarcomas [74], reflecting higher level of oxygenation and accounting for the higher radio-responsiveness. Kostourou *et al.* also demonstrated that a faster baseline R_2* was consistent with a greater vascular development [75]. Taylor *et al.* [76] reported results that are in contradiction with those reported by Rodrigues *et al.*[73]. They showed that tumor regions with fast R_2* stained positive with pimonidazole, a marker of radiobiologically significant tumor hypoxia. When incorporating relative blood volume map information, they observed no change in specificity of fast R_2* as a surrogate marker of tumor hypoxia. The study of Taylor *et al.* was conducted on patients with prostate cancer. It is possible that the blood volume fraction spatial distribution inside human tumors is quite homogeneous so that it might be a less predominant factor in determining regional R_2*.

Carbogen Stimulated BOLD MRI as a Method to Evaluate Tumor Hypoxia?

Following carbogen inhalation, spatial patterns of T_2* weighted signal enhancement can be very heterogeneous in tumors. For example, carbogen has relatively weak effects in hypoxic regions [77], because oxygenation would not be improved in poorly perfused areas (absence of vessels or vessel occlusion). Hence, poor or non-responding voxels could be used as a rule to assess the hypoxic fraction in tumors. A potential pitfall of this method is that changes in BOLD in well-perfused, highly oxic tumor areas would also show no significant BOLD signal changes, because hemoglobin is already largely in its oxygenated form. Nevertheless, Rodrigues *et al.* showed that carbogen-induced ΔR_2* is an informative parameter with respect to potential radiotherapeutic outcome [73]. A greater magnitude of the ΔR_2* response to carbogen was associated with a greater enhancement of the radiotherapeutic response. In their study, the magnitude of the response to carbogen was found to be determined by the mean perfused vascular fraction [74].

Other works provide evidence that tumor regions that exhibit higher pO_2 (and presumably are better perfused) give a larger BOLD response [49, 54].

To better understand which parameters could be inferred from magnitude of the BOLD response upon carbogen breathing, the BOLD MRI technique has been compared to dynamic contrast-enhanced (DCE) MRI after administration of contrast agent. Rijpkema *et al.* compared Gd-DTPA contrast enhanced MRI and BOLD MRI response for breathing of a $98\%O_2/2\%CO_2$ gas mixture in meningioma patients [78]. The pharmacokinetics of small paramagnetic contrast agents (Gd-DTPA) in tumors are influenced by vascular flow, blood volume and permeability surface area and extravascular extracellular space (EES) [79], so that DCE MRI results should be interpreted with caution. In their study, changes in T_2* was found to correlate negatively with kep - the rate constant between extravascular extracellular space (EES) and blood plasma [79]. Hence, tumors with a high T_2* response to hypercapnic hyperoxia tended to show low rates of tracer transport, suggesting that those tumors were per se less well perfused (assuming that perfusion is the dominant factor determining the kinetics of the contrast agent in the tumor). On the contrary, well-perfused tumors (associated with high values of kep) responded poorly upon carbogen breathing, presumably because hemoglobin is already for the most part in its oxygenated form. Interestingly, a positive correlation was found between changes in T_2* and the Δkep during hyperoxic gas challenge. So, tumors with non-significant increase or even negative change in T_2* showed a decrease in blood flow under hyperoxic hypercapnic conditions. Others have compared BOLD contrast in tumors and Gd-DTPA contrast enhanced imaging, but no correlation was found between the techniques. Peller *et al.* reported that the contrast enhancement on T_1 weighted images showed no correlation with the oxygen induced T_2* weighted signal intensity changes [80]. Similarly, Jiang *et al.* found a general lack of correlation between DCE and BOLD approaches in terms of maximum rate or magnitude of response in rat prostate tumor [81]. In these studies, however, a semiquantitative approach instead of pharmacokinetic modeling of tracer uptake could not truly have permitted across-subject comparison [79]. All together, these studies suggest that BOLD contrast in tumor in response to hyperoxic conditions is not uniquely interpretable in terms of tumor vascular architecture and oxygenation status.

APPLICATIONS

BOLD contrast MRI has been used to investigate parameters related to tumor vasculature such as perfusion, blood oxygenation, blood vessel development, remodeling and function. It has also been used to monitor the effects of anti-cancer therapy.

Monitoring Tumor Response to Vasomodulators

The sensitivity of BOLD contrast techniques to changes in tumor deoxyhemoglobin concentration is of relevance to many strategies in cancer treatments, particularly with regard to interventions designed to alter tumor oxygenation. The ability of the BOLD MRI technique to provide information on the time course of the effect of drug treatment on oxygenation of tumors can be used effectively to rationalize radiotherapy schema treatment. A number of adjuvant treatments have been designed to increase tissue oxygen tension in radioresistant tumor regions. One vascular intervention currently being assessed for its ability to improve tumor oxygenation prior to radiotherapy is carbogen ($95\%CO_2/5\%O_2$) breathing and nicotinamide in combination [82].

BOLD MRI has been reported as a very sensitive method to assess the variations of tumor oxygenation after hyperoxic gas breathing. This was first demonstrated in the pioneering studies of the group of Karczmar and Griffiths [83-85] and later applied by many groups in oncology [66, 67, 86-91].

Breathing high-oxygen content gases such as carbogen increases the amount of dissolved oxygen in the plasma, providing more oxygen at the capillary level and hence allowing diffusion of oxygen into hypoxic regions in order to radiosensitize them. The incorporation of 5% CO_2 is believed to counteract any oxygen-induced vasoconstriction. The increased blood oxygenation associated with carbogen breathing produces a decrease in R_2*. Similarly a decrease in the deoxyHb content of the tissue will also occur if there is an increase in blood flow, thereby reducing the fraction of oxygen extracted from the blood.

Other vasomodulators (improving or worsening oxygen delivery to tumor) have been studied using BOLD contrast MRI. Howe *et al.* measured the R_2* changes in a prolactinoma tumor model for a variety of vasoactive challenges (calcitonin gene related peptide, hydralazine, nicotinamide, carbogen and N_2 breathing) [52]. Frequently, R_2* decreased after treament with carbogen and nicotinamide, and increased after CGRP and hydralazine. However, concomitant changes in blood volume and changes in blood pH and metabolic status can lead to smaller-than-expected or even negative R_2* changes. For example, tumors showed a unexpected decrease in R_2* with 100% N_2 breathing, likely due to blood volume reduction because of a vascular collapse [52]. Also, acidification of blood during carbogen breathing could cause an increase in dHb due to the Bohr effect. Jordan *et al.* observed BOLD image intensity enhancement in murine fibrosarcoma upon nitric oxide donor isosorbide dinitrate treatment. This image enhancement was well correlated with an increase in tumor blood flow and pO_2 as demonstrated using Gd-DTPA contrast enhanced imaging and EPR oximetry, respectively [67]. Muruganandham *et al.* studied the hemodynamic changes induced by diltiazem, a calcium channel blocker with radiosensitizing properties, in tumor using BOLD MRI and Gd-DTPA DCE MRI techniques [92]. BOLD images showed signal enhancement upon diltiazem administration due to increase in tumor blood flow, assuming that diltiazem does not influence tumor cell oxygen consumption. Upon flunarizine treatment (calcium channel blocker), whole tumor averaged analysis revealed no change in BOLD image intensity, whereas a cluster analysis allowed observation of tumor regions with opposite patterns of response. These observations suggested that a "vascular steal" phenomenon (redistribution of blood flow) may have occurred [86]. Indeed, blood flow may be increased locally at the expense of an adjacent location, depending on the vascular bed [93].

Such results emphasize the importance of an assessment of the heterogeneity in tumor BOLD response upon treatment. Variable patterns of signal intensity changes have been observed using high oxygen content gas breathing. For example, Peller *et al.* [80] observed both positive and negative (up to 30% of all voxels) T_2* weighted signal intensity changes using 100% oxygen, while Karczmar and co-workers [83,94,95] reported negative changes in 2-15% of all voxels. Other studies illustrate the heterogeneous response to carbogen breathing in rodent tumor models [55,87,96]. Similarly, we identified discrete tumor regions that respond negatively to carbogen in the FSa fibrosarcoma tumor model [86]. Areas of reduced signal during carbogen breathing adjacent to tumor areas of increased signal have also been observed in some patients [89,97]. The occurrence of the steal effect likely depends on the structure of the intratumoral vasculature network and its relationship with normal host tissue. Information about the cause, the extent and the relevance of the steal effect is currently still limited. Further investigations will be needed to answer these questions.

The use of anesthetic agent can also affect BOLD signal intensity in a significant way. We observed that the signal intensity was dramatically decreased in the TLT tumor model after administration of pentobarbital, ketamine/xylazine or fentanyl/droperidol anesthetics, even if normothermia was maintained [98]. This signal decrease was not observed with isoflurane, however [90]. Drops in signal intensity correlated with measurements of oxygenation and blood perfusion using the Oxford OxyLite/OxyFlo fiberoptic probe system. Because of these potential caveats, particular care needs to be taken to monitor of the effects of anesthesia when trying to identify new therapeutic approaches that are aimed at modulating tumor hemodynamics. Core temperature can also influence tissue oxygen status and blood flow, thereby influencing BOLD contrast. The importance of monitoring core temperature during the imaging procedure has been described recently by Reijnders *et al.* [99]. In their study, they observed stronger enhancement in tumor signals upon carbogen inhalation at a core temperature of 30°C compared to the normal core temperature of 37°C [99].

Amorino *et al.* observed an increase in the BOLD signal ratio (suggesting a decrease in R_2*) of rodent tumor after administration of RSR13, an allosteric effector of hemoglobin [100]. BOLD MRI results support the reported RSR13-induced increase in tumor oxygenation obtained using pO_2 microelectrodes. RSR313 induces allosteric modification of hemoglobin, so that hemoglobin's binding affinity for oxygen is decreased, resulting in increased oxygen release from erythrocytes to tumor tissue [100,101]. Since the mechanism of tissue oxygenation by RSR13 involves an increase in deoxyhemoblobin levels, a decrease in the BOLD MRI signal after RSR13 administration might be expected. Amorino *et al.* hypothesized that a predominant T_1 effect due to molecular oxygen (RSR13 causes an increase in arterial oxygen tension), competing with the deoxyhemoblobin effect on T_2*, could explain the global increase in the MRI signal [100]. Later, Hou *et al.* showed that there was little impact of RSR13 on R_2* while an increase in oxygen in the tumor was still observed as measured using EPR oximetry [101]. The absence of change in R_2* suggests that tumor physiology remained constant. Using the Hill equation and the Krogh cylinder model, Hou *et al.* modeled the observed change in tumor pO_2 as a function of partial oxygen pressure at half-saturation of hemoglobin (P50) right shift due to RSR13, keeping oxygen saturation of blood, tumor blood flow and metabolic rate constant. The use of 100% oxygen breathing instead of air breathing during animal anesthesia can also explain the absence of detectable changes in R_2* as reported by Hou *et al.*, compared to the increase in BOLD signal ratio described by Amorino *et al.* Sufficient hemoglobin saturation with oxygen at the time of imaging could also explain the absence of drug effect.

Monitoring Photodynamic Therapy of Solid Tumors

Photodynamic therapy (PDT) has become an established cancer treatment that involves the interaction of a photosensitizer and light in an oxygenated environment [102]. Upon activation by light of a specific wavelength, the photosensitizing compound, localized in the tumor tissue, reacts with molecular oxygen, and generates cytotoxic reactive oxygen species, leading to tumor damage by killing tumor cells and/or tumor vasculature [102].

BOLD-contrast MRI may be a valuable tool for real-time monitoring of PDT efficacy. Gross *et al.* demonstrated that photoconsumption of oxygen and the consequent hemodynamic effects inherent to antivascular photodynamic therapy can generate BOLD contrast in tumors [103]. A rapid decline in relative signal intensity in T_2* weighted images (25-40%) and a rapid increase in ΔR_2* were observed upon intravascular photosensitization. It was demonstrated that the observed changes in BOLD contrast were the result of two processes closely related in time. First, the rapid photochemical oxygen consumption leads to a decline in hemoglobin saturation levels as observed using *in vitro* spectral analysis. Second, an intense reduction in tumor blood vessel perfusion, reaching stasis, takes place as revealed by fluorescence intravital microscopy. It should be noted that PDT can deplete or enhance tumor oxygenation, depending on the choice of photosensitizer, drug-light interval, or fluence rate [104-106]. The oxygen-favoring photodynamic protocol may be desired to enhance radiation sensitivity [107], while antivascular PDT is crucial for development of necrosis and tumor eradication [102]. Whatever the protocol, *in vivo* monitoring of photodynamic therapy induced changes in tumor oxygenation and perfusion is of great clinical significance as it can provide a valuable prognostic indicator [108].

Angiogenesis and Maturation of Vessels

Histologic assays of angiogenesis based on microvascular density (MVD) is a common method for characterizing the vascular bed of tumors [109]. Studies have revealed that high MVD counts within vascular hot spots of tumors correspond with a poor prognosis [110]. While MVD is a useful surrogate of angiogenesis, the method has many drawbacks such as invasiveness and low reproducibility among pathologists. MRI, with its high temporal and spatial resolution, is an ideal technique for noninvasive assay of tumor angiogenesis *in vivo*. Susceptibility contrast-enhanced

MRI after administration of contrast agent is increasingly being used in this regard [111]. Alternatively, *intrinsic* susceptibility-based MRI, which is sensitive to changes in endogenous deoxyhemoglobin, can provide a complementary approach. R_2* is directly proportional to the tissue content of deoxyhemoglobin and hence is a sensitive index of tissue vascularity. A fast R_2* is consistent with a high concentration of deoxyhemoglobin and hence indicative of high blood vessel density, although cellular paramagnetic debris from necrosis such as hemosiderin can also increase R_2*. The rise in vessel density, upon stimulation of angiogenesis, has an overwhelming effect (signal loss) on GRE contrast in images of the subcutaneous vasculature [112]. In addition, there was a highly significant correlation between vessel density determined by MRI and vessel density determined immediately postmortem from skin specimens [112]. The method has great potential for basic research of the regulation of tumor angiogenesis and wound healing and for evaluation of promoters of angiogenesis and antiangiogenic therapies [75,113,114].

Analyzing the functional properties of the tumor vascular bed would more realistically assess the angiogenic status of the vasculature than the presence of blood vessels alone. A number of immunohistochemical techniques are available to assess the function of tumor vasculature at a microscopic level [115]. Alternatively, monitoring of dynamic changes in GRE images or R_2* in response to hypercapnia and hyperoxia can be used to probe non-invasively the maturation and functional state (perfusion status of the vessels) of the tumor vasculature. For carbogen breathing, acute changes in systemic blood oxygenation are expected to occur in the functional (capable of erythrocyte-mediated oxygen delivery) vascular bed. As mentioned above, the approach of the functionality mapping technique using *hyperoxia* would, however, not be valid in well-oxygenated organs where arterial HbO_2 is already fully oxygenated (generally not the case for tumor tissues). MR assessment of perfusion status of the tumor (fraction of functional vessels) can be used to monitor non-invasively the damages of the vascular bed after anti-vascular or anti-angiogenic therapy. Furthermore, the amplitude of the MR response can be viewed as an assessment of apparent vessel density (with high values corresponding to high vessel density) [74] and can be used, for example, for the monitoring of vascular remodeling during tumor growth [116]. Thomas *et al.* recently demonstrated a link between tumour growth rates and tumour fractions exhibiting signal increase upon carbogen breathing for a chemically induced hepatocellular carcinoma in mice [90,91].

On the other hand, BOLD MRI during hypercapnia (elevation of inhaled CO_2) can reflect varying degrees of maturation of the tumor vascular bed [116,117]. Microcapillary maturation is a progressive process in tumors. It requires a mix of angio- and arteriogenic factors for a sufficient duration so that nascent vessels can tighten up and become invested with pericytes -pericytes are contractile cells containing α-smooth muscle actin and desmin that stabilize vessel walls and participate in the regulation of the blood flow in the microcirculation. Consequently, vasoreactivity secondary to hypercapnia stress is not expected to occur in immature neovessels lacking smooth muscle cells by which the effects of elevated arterial CO_2 are mediated.

It has been demonstrated that, in extracerebral tumors, the MRI signal enhancement due to hypercapnia is the result of a change in the apparent T_1 relaxation due to an increased inflow. Parallel studies using intravital microscopy showed that hypercapnia induced vasoconstriction in mature vessels and a reduced red blood cell (RBC) flux and density[117]. The discrepancy in flow between MRI and intravital microscopy is consistent with increased *plasma* flow and reduced hematocrit. The drop in hematocrit will result in T_2* dependent increase of MRI signal intensity while increased plasma flow can enhance signal intensity by changing the apparent T_1 (inflow effect).

In vivo MR monitoring of the fraction of mature vessels can be used to predict the vascular response to antiangiogenic or anti-vascular treatments. Tumors with higher fraction of pericyte-covered mature vessels should be less susceptible to anti-angiogenic or anti-vascular therapy [118,119]. By using the MR approach, Abramovitch *et al.* demonstrated the selective destruction of immature vessels in response to VEGF withdrawal [120]. The inhibitory effect on vessel maturation of antiangiogenic compounds such as halofuginone or linomide have also been reported [114,120,121]. Another application could be the assessment of vascular maturation during proangiogenic therapy, which could be viewed as a marker for vascular stabilization. Hypercapnia challenges has also been applied for clinical evaluation of cerebrovascular response in patients with cerebral gliomas [122]. Several studies show that there is an increase in BOLD signal in the gray matter during hypercapnia [123,124]. Elevated arterial CO_2 tension due to hypercapnia challenge induces vasodilatation effects and causes cerebral blood flow increases. Hsu *et al.* showed that during short periods of breath holding, there was an absence of signal change in the bulk of the tumor, in contrast with the significant BOLD signal increases in normal appearing gray matter [122]. This lack of enhancement in hypoperfused regions could result from reduced local hematocrit due to decreased perfusion. The undetectability of BOLD signal changes in hyperperfused tumor regions could be due to masking of the effect of increased blood perfusion by the more prominent O_2 consumption. Decreases in BOLD signal were observed in high-grade gliomas, but not in the low-grade gliomas. The so-called steal phenomenon, redistribution of blood flow to a responsive tumor region and surrounding normal tissue, causing a focal worsening of tumor perfusion, is expected to be exaggerated in tumor regions were neovascularity is present.

Mapping Tumor Acute Hypoxia

Historically, tumor hypoxia has been thought to be dominated by diffusion limitations of oxygen. Intermittent hypoxia, on the other hand, has generally been thought to be less prominent and therefore less important than diffusion limited hypoxia. Evidence have been provided showing that tumor oxygenation is rarely at steady state, except perhaps at the extreme limit of the oxygen diffusion distance [11]. Instead, the oxygenation state is characterized by large temporal variations in pO_2, brought on by fluctuations in microvessel red cell flux [125]. Several factors may

contribute to flow fluctuations, including arteriolar vasomotion [10,11], rapid vascular modeling [12], and other hemodynamic effects such as non linear flow properties of blood or non-uniform axial distribution of red blood cells partitioning at bifurcations [126]. Acute hypoxia may be an under-appreciated therapeutic problem as it can be associated with resistance to radiation therapy [127-131], impaired delivery of chemotherapeutic agents [37], or metastasis development [132]. Studies carried out to assess the dynamic aspects of the fluctuating hypoxia use invasive techniques having poor spatial resolution (implantable laser Doppler probes [133,134], O_2 electrodes [125,133], OxyLite sensors [135] or intravital microscopy techniques [10,11,133]) and therefore limit the potential of investigation of the phenomenon. In a recent study, we demonstrated that T_2* weighted gradient-echo MRI could provide an alternative non-invasive technique to uncover transient fluctuations of blood flow and/or oxygenation [136]. Anesthetized FSa tumor-bearing mice were continuously imaged during 30-min sampling periods. By subjecting the time-dependent data to power spectrum analysis we identified voxels with statistically significant spontaneous basal MR signal fluctuations (see Fig. **5**). Dynamic changes in T_2* were also tracked using multiple GRE imaging. The cycle time of the fluctuations were characterized by low frequencies, ranging from 1 cycle/1h to 1 cycle/3min, which were similar to cycle times of fluctuations in tumor blood flow and oxygen as reported previously by using alternative techniques. No obvious temporal correlation was found between muscle and tumor fluctuations. Our data showed that the fluctuating tumor zones were predominantly located in regions with functional vessels. In addition, we observed that the method was suitable to monitor areas of tumors that were sensitive to treatments designed to decrease the occurrence of tumor acute hypoxia (see Fig. **6**). Further studies will be required to understand whether spontaneous fluctuations of blood flow and/or oxygenation as observed using the BOLD MRI are of prognostic indicator of radiotherapy or chemotherapy resistance.

BOLD MRI: THE GOOD, THE BAD AND THE UGLY

As with any technique, BOLD MRI has both advantages and disadvantages. One advantage of BOLD MRI is that it is non-invasive and can be used to monitor real time changes of tumor oxygenation during pharmacological treatments or other treatments such as photodynamic therapy. BOLD MRI also has high spatial resolution, allowing it to address the issue of the spatial heterogeneity of the tumor response. Carbogen induced changes in R_2* or basal R_2*, which reflect vascular development, may also be monitored with BOLD MRI to predict radiotherapy sensitivity. BOLD MRI, in combination with hypercapnia and hyperoxia, is also an attractive method for assessing maturation and the functional state of the tumor. Another appealing application is the study of changes in blood flow and oxygenation associated with the phenomenon of fluctuating hypoxia.

As for disadvantages, BOLD MRI is unfortunately a non-quantitative method for monitoring tumor pO_2. This is the result of the extreme sensitivity of changes in R_2* to the basal state of tumor oxygenation and blood volume fraction. The intra- and inter-tumoral distribution of these parameters may be greatly heterogeneous, making it very difficult to compare estimated pO_2 changes between two regions or individuals. Even more problematic is the fact that the change in R_2* is not always indicative of the change in pO_2. Concomitant changes in blood volume, blood pH and metabolic status can lead to smaller-than-expected or even negative changes in R_2*.

In conclusion, when applied properly, BOLD MRI has become a useful tool for addressing important questions regarding the pathophysiology and treatments of tumors.

ABBREVIATIONS

R_2, R_2*	=	Transverse and apparent transverse relaxation rates
T_2, T_2*	=	Transverse and apparent transverse relaxation times

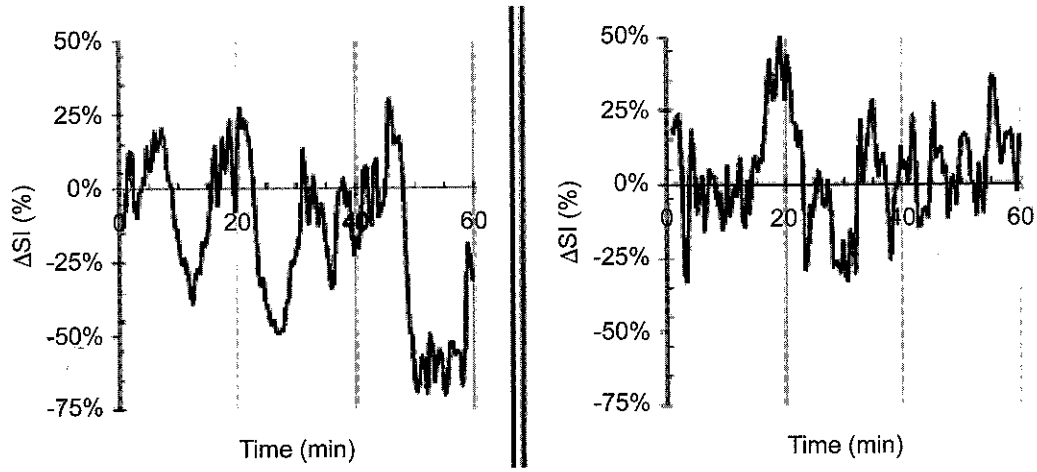

Fig. (5). Typical examples of spontaneous T_2*-weighted signal fluctuations in the tumor during air breathing. Data presented are single voxel signals. *Adapted from ref [136].*

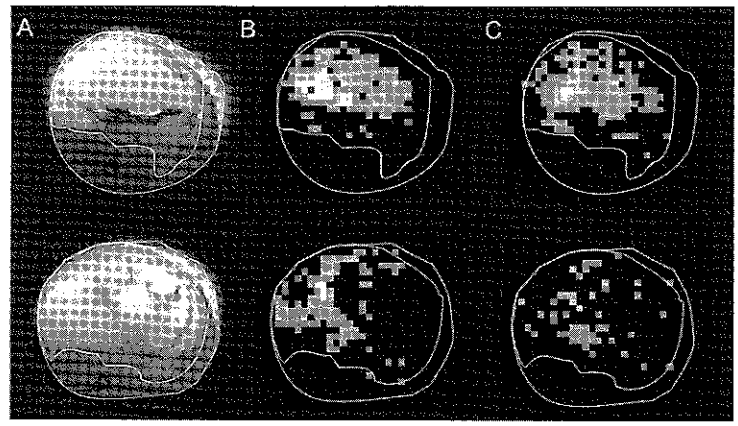

Fig. (6). (A). T_2-weighted anatomical images of a FSa tumor (mouse leg and tumor borders are delineated). Maps of spontaneous T_2*-weighted signal fluctuations inside the tumor over a 30 min sampling period pre (B) and 30 min post treatment (C). Upper: control mouse, Lower: effect of carbogen breathing and nicotinamide administration (note the decrease in the number of fluctuating voxels). *Adapted from ref [136].*

GRE MRI = Gradient-recalled echo magnetic resonance imaging

dHb = Deoxyhemoglobin

REFERENCES

[1] Vaupel P, Harrison L. Tumor hypoxia: causative factors, compensatory mechanisms, and cellular response. Oncologist 2004; 9 Suppl 5: 4-9.

[2] Munn LL. Aberrant vascular architecture in tumors and its importance in drug-based therapies. Drug Discov Today 2003; 8: 396-403.

[3] Hashizume H, Baluk P, Morikawa S, *et al.* Openings between defective endothelial cells explain tumor vessel leakiness. Am J Pathol 2000; 156: 1363-80.

[4] McDonald DM, Baluk P. Significance of blood vessel leakiness in cancer. Cancer Res 2002; 62: 5381-5.

[5] Gatenby RA, Gillies RJ. Why do cancers have high aerobic glycolysis? Nat Rev Cancer 2004; 4: 891-9.

[6] Dewhirst MW. Concepts of oxygen transport at the microcirculatory level. Semin Radiat Oncol 1998; 8: 143-50.

[7] Thomlinson RH, Gray LH. The histological structure of some human lung cancers and the possible implications for radiotherapy. Br J Cancer 1955; 9: 539-49.

[8] Erickson K, Braun RD, Yu D, *et al.* Effect of longitudinal oxygen gradients on effectiveness of manipulation of tumor oxygenation. Cancer Res 2003; 63: 4705-12.

[9] Secomb TW, Hsu R, Braun RD, *et al.* Theoretical simulation of oxygen transport to tumors by three-dimensional networks of microvessels. Adv Exp Med Biol 1998; 454: 629-34.

[10] Intaglietta M, Myers RR, Gross JF, Reinhold HS. Dynamics of microvascular flow in implanted mouse mammary tumours. Bibl Anat 1977; 15: 273-6.

[11] Dewhirst MW, Kimura H, Rehmus SW, *et al.* Microvascular studies on the origins of perfusion-limited hypoxia. Br J Cancer Suppl 1996; 27:S247-S251.

[12] Patan S, Munn LL, Jain RK. Intussusceptive microvascular growth in a human colon adenocarcinoma xenograft: a novel mechanism of tumor angiogenesis. Microvasc Res 1996; 51: 260-72.

[13] Kiani MF, Pries AR, Hsu LL, Sarelius IH, Cokelet GR. Fluctuations in microvascular blood flow parameters caused by hemodynamic mechanisms. Am J Physiol 1994; 266: H1822-H1828.

[14] Mollica F, Jain RK, Netti PA. A model for temporal heterogeneities of tumor blood flow. Microvasc Res 2003; 65: 56-60.

[15] Rofstad EK. Microenvironment-induced cancer metastasis. Int J Radiat Biol 2000; 76: 589-605.

[16] Young SD, Marshall RS, Hill RP. Hypoxia induces DNA overreplication and enhances metastatic potential of murine tumor cells. Proc Natl Acad Sci USA 1988; 85: 9533-7.

[17] Rofstad EK, Danielsen T. Hypoxia-induced metastasis of human melanoma cells: involvement of vascular endothelial growth factor-mediated angiogenesis. Br J Cancer 1999; 80: 1697-707.

[18] Cairns RA, Hill RP. Acute hypoxia enhances spontaneous lymph node metastasis in an orthotopic murine model of human cervical carcinoma. Cancer Res 2004; 64: 2054-61.

[19] Graeber TG, Osmanian C, Jacks T, *et al.* Hypoxia-mediated selection of cells with diminished apoptotic potential in solid tumours. Nature 1996; 379: 88-91.

[20] Hockel M, Schlenger K, Hockel S, Vaupel P. Hypoxic cervical cancers with low apoptotic index are highly aggressive. Cancer Res 1999; 59: 4525-8.

[21] Semenza GL. Regulation of hypoxia-induced angiogenesis: a chaperone escorts VEGF to the dance. J Clin Invest 2001; 108: 39-40.

[22] Wenger RH. Cellular adaptation to hypoxia: O2-sensing protein hydroxylases, hypoxia-inducible transcription factors, and O2-regulated gene expression. FASEB J 2002; 16: 1151-62.

[23] Semenza GL. Targeting HIF-1 for cancer therapy. Nat Rev Cancer 2003; 3: 721-32.

[24] Harrison L, Blackwell K. Hypoxia and anemia: factors in decreased sensitivity to radiation therapy and chemotherapy? Oncologist 2004; 9 Suppl 5: 31-40.

[25] Gray LH, Conger AD, Ebert M, Hornsey S, Scott OC. The concentration of oxygen dissolved in tissues at the time of irradiation as a factor in radiotherapy. Br J Radiol 1953; 26: 638-48.

[26] Gatenby RA, Kessler HB, Rosenblum JS, *et al.* Oxygen distribution in squamous cell carcinoma metastases and its relationship to outcome of radiation therapy. Int J Radiat Oncol Biol Phys 1988; 14: 831-8.

[27] Hockel M, Schlenger K, Mitze M, Schaffer U, Vaupel P. Hypoxia and Radiation Response in Human Tumors. Semin Radiat Oncol 1996; 6: 3-9.

[28] Okunieff P, Hoeckel M, Dunphy EP, *et al.* Oxygen tension distributions are sufficient to explain the local response of human breast tumors treated with radiation alone. Int J Radiat Oncol Biol Phys 1993; 26: 631-6.

[29] Stone HB, Brown JM, Phillips TL, Sutherland RM. Oxygen in human tumors: correlations between methods of measurement and response to therapy. Summary of a workshop held November 19-20, 1992, at the National Cancer Institute, Bethesda, Maryland. Radiat Res 1993; 136: 422-34.

[30] Thomas CD, Chavaudra N, Martin L, Guichard M. Correlation between radiosensitivity, percentage hypoxic cells and pO2 measurements in one rodent and two human tumor xenografts. Radiat Res 1994; 139: 1-8.

[31] O'Hara JA, Goda F, Demidenko E, Swartz HM. Effect on regrowth delay in a murine tumor of scheduling split-dose irradiation based on direct pO2 measurements by electron paramagnetic resonance oximetry. Radiat Res 1998; 150: 549-56.

[32] O'Hara JA, Blumenthal RD, Grinberg OY, *et al.* Response to radioimmunotherapy correlates with tumor pO2 measured by EPR oximetry in human tumor xenografts. Radiat Res 2001; 155: 466-73.

[33] Zhao D, Constantinescu A, Chang CH, Hahn EW, Mason RP. Correlation of tumor oxygen dynamics with radiation response of the dunning prostate R3327-HI tumor. Radiat Res 2003; 159: 621-31.

[34] Shannon AM, Bouchier-Hayes DJ, Condron CM, Toomey D. Tumour hypoxia, chemotherapeutic resistance and hypoxia-related therapies. Cancer Treat Rev 2003; 29: 297-307.

[35] Durand RE. The influence of microenvironmental factors during cancer therapy. *In Vivo* 1994; 8: 691-702.

[36] Denny WA. Prospects for hypoxia-activated anticancer drugs. Curr Med Chem Anti -Canc Agents 2004; 4: 395-9.

[37] Durand RE. Intermittent blood flow in solid tumours--an under-appreciated source of 'drug resistance'. Cancer Metastasis Rev 2001; 20: 57-61.

[38] Heffer E, Pera V, Schutz O, Siebold H, Fantini S. Near-infrared imaging of the human breast: complementing hemoglobin concentration maps with oxygenation images. J Biomed Opt 2004; 9: 1152-60.

[39] Ballinger JR. Imaging hypoxia in tumors. Semin Nucl Med 2001; 31: 321-9.

[40] Gambhir SS. Molecular imaging of cancer with positron emission tomography. Nat Rev Cancer 2002; 2: 683-93.

[41] Gallez B, Baudelet C, Jordan BF. Assessment of tumor oxygenation by electron paramagnetic resonance: principles and applications. NMR Biomed 2004; 17: 240-62.

[42] Grucker D. Oxymetry by magnetic resonance: applications to animal biology and medicine. Progress in Nuclear Magnetic Resonance Spectroscopy 2000; 36: 241-70.

[43] Robinson SP, Griffiths JR. Current issues in the utility of 19F nuclear magnetic resonance methodologies for the assessment of tumour hypoxia. Philos Trans R Soc Lond B Biol Sci 2004; 359: 987-96.

[44] Zhao D, Jiang L, Mason RP. Measuring changes in tumor oxygenation. Methods Enzymol 2004; 386: 378-418.

[45] Hennig J, Speck O, Koch MA, Weiller C. Functional magnetic resonance imaging: a review of methodological aspects and clinical applications. J Magn Reson Imaging 2003; 18: 1-15.

[46] Ogawa S, Lee TM. Magnetic resonance imaging of blood vessels at high fields: *in vivo* and *in vitro* measurements and image simulation. Magn Reson Med 1990; 16: 9-18.

[47] Thulborn KR, Waterton JC, Matthews PM, Radda GK. Oxygenation dependence of the transverse relaxation time of water protons in whole blood at high field. Biochim Biophys Acta 1982; 714: 265-70.

[48] Boxerman JL, Hamberg LM, Rosen BR, Weisskoff RM. MR contrast due to intravascular magnetic susceptibility perturbations. Magn Reson Med 1995; 34: 555-66.

[49] Baudelet C, Gallez B. How does blood oxygen level-dependent (BOLD) contrast correlate with oxygen partial pressure (pO2) inside tumors? Magn Reson Med 2002; 48: 980-6.

[50] Li D, Wang Y, Waight DJ. Blood oxygen saturation assessment *in vivo* using T2* estimation. Magn Reson Med 1998; 39: 685-90.

[51] Duyn JH, Moonen CT, van Yperen GH, de Boer RW, Luyten PR. Inflow versus deoxyhemoglobin effects in BOLD functional MRI using gradient echoes at 1. 5 T. NMR Biomed 1994; 7: 83-8.

[52] Howe FA, Robinson SP, McIntyre DJ, Stubbs M, Griffiths JR. Issues in flow and oxygenation dependent contrast (FLOOD) imaging of tumours. NMR Biomed 2001; 14: 497-506.

[53] Lebon V, Carlier PG, Brillault-Salvat C, Leroy-Willig A. Simultaneous measurement of perfusion and oxygenation changes using a multiple gradient-echo sequence: application to human muscle study. Magn Reson Imaging 1998; 16: 721-9.

[54] Fan X, River JN, Zamora M, al Hallaq HA, Karczmar GS. Effect of carbogen on tumor oxygenation: combined fluorine-19 and proton MRI measurements. Int J Radiat Oncol Biol Phys 2002; 54: 1202-9.

[55] al Hallaq HA, Fan X, Zamora M, *et al.* Spectrally inhomogeneous BOLD contrast changes detected in rodent tumors with high spectral and spatial resolution MRI. NMR Biomed 2002; 15: 28-36.

[56] al Hallaq HA, Zamora MA, Fish BL, *et al.* Using high spectral and spatial resolution bold MRI to choose the optimal oxygenating treatment for individual cancer patients. Adv Exp Med Biol 2003; 530: 433-40.

[57] Dixon WT. Simple proton spectroscopic imaging. Radiology 1984; 153: 189-94.

[58] Glover GH. Multipoint Dixon technique for water and fat proton and susceptibility imaging. J Magn Reson Imaging 1991; 1: 521-30.

[59] Kovar DA, al Hallaq HA, Zamora MA, River JN, Karczmar GS. Fast spectroscopic imaging of water and fat resonances to improve the quality of MR images. Acad Radiol 1998; 5: 269-75.

[60] Jensen FB. Red blood cell pH, the Bohr effect, and other oxygenation-linked phenomena in blood O2 and CO2 transport. Acta Physiol Scand 2004; 182: 215-27.

[61] Snyder SA, Lanzen JL, Braun RD, *et al.* Simultaneous administration of glucose and hyperoxic gas achieves greater improvement in tumor oxygenation than hyperoxic gas alone. Int J Radiat Oncol Biol Phys 2001; 51: 494-506.

[62] Stubbs M, Robinson SP, Rodrigues LM, *et al.* The effects of host carbogen (95% oxygen/5% carbon dioxide) breathing on metabolic characteristics of Morris hepatoma 9618a. Br J Cancer 1998; 78: 1449-56.

[63] Robinson SP, Collingridge DR, Howe FA, *et al.* Tumour response to hypercapnia and hyperoxia monitored by FLOOD magnetic resonance imaging. NMR Biomed 1999; 12: 98-106.

[64] al Hallaq HA, River JN, Zamora M, Oikawa H, Karczmar GS. Correlation of magnetic resonance and oxygen microelectrode measurements of carbogen-induced changes in tumor oxygenation. Int J Radiat Oncol Biol Phys 1998; 41: 151-9.

[65] Hoppel BE, Weisskoff RM, Thulborn KR, *et al.* Measurement of regional blood oxygenation and cerebral hemodynamics. Magn Reson Med 1993; 30: 715-23.

[66] Dunn JF, O'Hara JA, Zaim-Wadghiri Y, *et al.* Changes in oxygenation of intracranial tumors with carbogen: a BOLD MRI and EPR oximetry study. J Magn Reson Imaging 2002; 16: 511-21.

[67] Jordan BF, Misson P, Demeure R, *et al.* Changes in tumor oxygenation/perfusion induced by the no donor, isosorbide dinitrate, in comparison with carbogen: monitoring by EPR and MRI. Int J Radiat Oncol Biol Phys 2000; 48: 565-70.

[68] Williams BB, al Hallaq H, Chandramouli GV, *et al.* Imaging spin probe distribution in the tumor of a living mouse with 250 MHz EPR: correlation with BOLD MRI. Magn Reson Med 2002; 47: 634-8.

[69] Elas M, Williams BB, Parasca A, *et al.* Quantitative tumor oxymetric images from 4D electron paramagnetic resonance imaging (EPRI): methodology and comparison with blood oxygen level-dependent (BOLD) MRI. Magn Reson Med 2003; 49: 682-91.

[70] Demeure RJ, Jordan BF, Yang QX, *et al.* Removal of local field gradient artefacts in BOLD contrast imaging of head and neck tumours. Phys Med Biol 2002; 47: 1819-25.

[71] Frahm J, Merboldt KD, Hanicke W. Direct FLASH MR imaging of magnetic field inhomogeneities by gradient compensation. Magn Reson Med 1988; 6: 474-80.

[72] Stenger VA, Boada FE, Noll DC. Three-dimensional tailored RF pulses for the reduction of susceptibility artifacts in T(*)(2)-weighted functional MRI. Magn Reson Med 2000; 44: 525-31.

[73] Rodrigues LM, Howe FA, Griffiths JR, Robinson SP. Tumor R2* is a prognostic indicator of acute radiotherapeutic response in rodent tumors. J Magn Reson Imaging 2004; 19: 482-8.

[74] Robinson SP, Rijken PF, Howe FA, *et al.* Tumor vascular architecture and function evaluated by non-invasive susceptibility MRI methods and immunohistochemistry. J Magn Reson Imaging 2003; 17: 445-54.

[75] Kostourou V, Robinson SP, Whitley GS, Griffiths JR. Effects of overexpression of dimethylarginine dimethylaminohydrolase on tumor angiogenesis assessed by susceptibility magnetic resonance imaging. Cancer Res 2003; 63: 4960-6.

[76] Taylor NJ, Carnell DM, Smith RE, *et al.* Evaluation of prostate gland hypoxia with quantified BOLD MRI: initial results from a

correlated histological study. Proc Intl Soc Mag Reson Med 2003; 11:531.

[77] Fan X, River JN, Zamora M, al Hallaq HA, Karczmar GS. Effect of carbogen on tumor oxygenation: combined fluorine-19 and proton MRI measurements. Int J Radiat Oncol Biol Phys 2002; 54: 1202-9.

[78] Rijpkema M, Schuuring J, Bernsen PL, *et al.* BOLD MRI response to hypercapnic hyperoxia in patients with meningiomas: correlation with Gadolinium-DTPA uptake rate. Magn Reson Imaging 2004; 22: 761-7.

[79] Tofts PS, Brix G, Buckley DL, *et al.* Estimating kinetic parameters from dynamic contrast-enhanced T(1)-weighted MRI of a diffusable tracer: standardized quantities and symbols. J Magn Reson Imaging 1999; 10: 223-32.

[80] Peller M, Weissfloch L, Stehling MK, *et al.* Oxygen-induced MR signal changes in murine tumors. Magn Reson Imaging 1998; 16: 799-809.

[81] Jiang L, Zhao D, Constantinescu A, Mason RP. Comparison of BOLD contrast and Gd-DTPA dynamic contrast-enhanced imaging in rat prostate tumor. Magn Reson Med 2004; 51: 953-60.

[82] Kaanders JH, Bussink J, van der Kogel AJ. ARCON: a novel biology-based approach in radiotherapy. Lancet Oncol 2002; 3: 728-37.

[83] Karczmar GS, Kuperman VY, River JN, Lewis MZ, Lipton MJ. Magnetic resonance measurement of response to hyperoxia differentiates tumors from normal tissue and may be sensitive to oxygen consumption. Invest Radiol 1994; 29 Suppl 2:S161-S163.

[84] Kuperman VY, River JN, Lewis MZ, Lubich LM, Karczmar GS. Changes in T2*-weighted images during hyperoxia differentiate tumors from normal tissue. Magn Reson Med 1995; 33: 318-25.

[85] Robinson SP, Howe FA, Griffiths JR. Noninvasive monitoring of carbogen-induced changes in tumor blood flow and oxygenation by functional magnetic resonance imaging. Int J Radiat Oncol Biol Phys 1995; 33: 855-9.

[86] Baudelet C, Gallez B. Cluster analysis of BOLD fMRI time series in tumors to study the heterogeneity of hemodynamic response to treatment. Magn Reson Med 2003; 49: 985-90.

[87] Landuyt W, Hermans R, Bosmans H, *et al.* BOLD contrast fMRI of whole rodent tumour during air or carbogen breathing using echo-planar imaging at 1. 5 T. Eur Radiol 2001; 11: 2332-40.

[88] Rijpkema M, Kaanders JH, Joosten FB, van der Kogel AJ, Heerschap A. Effects of breathing a hyperoxic hypercapnic gas mixture on blood oxygenation and vascularity of head-and-neck tumors as measured by magnetic resonance imaging. Int J Radiat Oncol Biol Phys 2002; 53: 1185-91.

[89] Taylor NJ, Baddeley H, Goodchild KA, *et al.* BOLD MRI of human tumor oxygenation during carbogen breathing. J Magn Reson Imaging 2001; 14: 156-63.

[90] Thomas CD, Chenu E, Walczak C, *et al.* Morphological and carbogen-based functional MRI of a chemically induced liver tumor model in mice. Magn Reson Med 2003; 50: 522-30.

[91] Thomas CD, Chenu E, Walczak C, *et al.* Relationship between tumour growth rate and carbogen-based functional MRI for a chemically induced HCC in mice. MAGMA 2004.

[92] Muruganandham M, Kasiviswanathan A, Jagannathan NR, *et al.* Diltiazem enhances tumor blood flow: MRI study in a murine tumor. Int J Radiat Oncol Biol Phys 1999; 43: 413-21.

[93] Zlotecki RA, Baxter LT, Boucher Y, Jain RK. Pharmacologic modification of tumor blood flow and interstitial fluid pressure in a human tumor xenograft: network analysis and mechanistic interpretation. Microvasc Res 1995; 50: 429-43.

[94] Karczmar GS, River JN, Li J, *et al.* Effects of hyperoxia on T2* and resonance frequency weighted magnetic resonance images of rodent tumours. NMR Biomed 1994; 7: 3-11.

[95] Kuperman VY, River JN, Lewis MZ, Lubich LM, Karczmar GS. Changes in T2*-weighted images during hyperoxia differentiate tumors from normal tissue. Magn Reson Med 1995; 33: 318-25.

[96] Robinson SP, Rodrigues LM, Ojugo AS, *et al.* The response to carbogen breathing in experimental tumour models monitored by gradient-recalled echo magnetic resonance imaging. Br J Cancer 1997; 75: 1000-6.

[97] Griffiths JR, Taylor NJ, Howe FA, *et al.* The response of human tumors to carbogen breathing, monitored by Gradient-Recalled Echo Magnetic Resonance Imaging. Int J Radiat Oncol Biol Phys 1997; 39: 697-701.

[98] Baudelet C, Gallez B. Effect of anesthesia on the signal intensity in tumors using BOLD-MRI: comparison with flow measurements by Laser Doppler flowmetry and oxygen measurements by luminescence-based probes. Magn Reson Imaging 2004; 22: 905-12.

[99] Reijnders K, English SJ, Krishna MC, *et al.* Influence of body temperature on the BOLD effect in murine SCC tumors. Magn Reson Med 2004; 51: 389-93.

[100] Amorino GP, Lee H, Holburn GE, *et al.* Enhancement of tumor oxygenation and radiation response by the allosteric effector of hemoglobin, RSR13. Radiat Res 2001; 156: 294-300.

[101] Hou H, Khan N, O'Hara JA, *et al.* Effect of RSR13, an allosteric hemoglobin modifier, on oxygenation in murine tumors: An *in vivo* electron paramagnetic resonance oximetry and bold MRI study. Int J Radiat Oncol Biol Phys 2004; 59: 834-43.

[102] Dolmans DE, Fukumura D, Jain RK. Photodynamic therapy for cancer. Nat Rev Cancer 2003; 3: 380-7.

[103] Gross S, Gilead A, Scherz A, Neeman M, Salomon Y. Monitoring photodynamic therapy of solid tumors online by BOLD-contrast MRI. Nat Med 2003; 9: 1327-31.

[104] Henderson BW, Busch TM, Vaughan LA, *et al.* Photofrin photodynamic therapy can significantly deplete or preserve oxygenation in human basal cell carcinomas during treatment, depending on fluence rate. Cancer Res 2000; 60: 525-9.

[105] Pogue BW, O'Hara JA, Goodwin IA, *et al.* Tumor PO(2) changes during photodynamic therapy depend upon photosensitizer type and time after injection. Comp Biochem Physiol A Mol Integr Physiol 2002; 132: 177-84.

[106] Sitnik TM, Hampton JA, Henderson BW. Reduction of tumour oxygenation during and after photodynamic therapy *in vivo*: effects of fluence rate. Br J Cancer 1998; 77: 1386-94.

[107] Pogue BW, O'Hara JA, Demidenko E, *et al.* Photodynamic therapy with verteporfin in the radiation-induced fibrosarcoma-1 tumor causes enhanced radiation sensitivity. Cancer Res 2003; 63: 1025-33.

[108] Wang HW, Putt ME, Emanuele MJ, *et al.* Treatment-induced changes in tumor oxygenation predict photodynamic therapy outcome. Cancer Res 2004; 64: 7553-61.

[109] Tozer GM. Measuring tumour vascular response to antivascular and antiangiogenic drugs. Br J Radiol 2003; 76 Spec No 1:S23-S35.

[110] Leek RD. The prognostic role of angiogenesis in breast cancer. Anticancer Res 2001; 21: 4325-31.

[111] Brasch R, Turetschek K. MRI characterization of tumors and grading angiogenesis using macromolecular contrast media: status report. Eur J Radiol 2000; 34: 148-55.

[112] Abramovitch R, Frenkiel D, Neeman M. Analysis of subcutaneous angiogenesis by gradient echo magnetic resonance imaging. Magn Reson Med 1998; 39: 813-24.

[113] Abramovitch R, Dafni H, Neeman M, Nagler A, Pines M. Inhibition of neovascularization and tumor growth, and facilitation of wound repair, by halofuginone, an inhibitor of collagen type I synthesis. Neoplasia 1999; 1: 321-9.

[114] Abramovitch R, Itzik A, Harel H, *et al.* Halofuginone inhibits angiogenesis and growth in implanted metastatic rat brain tumor model--an MRI study. Neoplasia 2004; 6: 480-9.

[115] Fox SB, Harris AL. Histological quantitation of tumour angiogenesis. APMIS 2004; 112: 413-30.

[116] Gilead A, Meir G, Neeman M. The role of angiogenesis, vascular maturation, regression and stroma infiltration in dormancy and growth of implanted MLS ovarian carcinoma spheroids. Int J Cancer 2004; 108: 524-31.

[117] Neeman M, Dafni H, Bukhari O, Braun RD, Dewhirst MW. *In vivo* BOLD contrast MRI mapping of subcutaneous vascular function and maturation: validation by intravital microscopy. Magn Reson Med 2001; 45: 887-98.

[118] Gee MS, Procopio WN, Makonnen S, *et al.* Tumor vessel development and maturation impose limits on the effectiveness of anti-vascular therapy. Am J Pathol 2003; 162: 183-93.

[119] Eberhard A, Kahlert S, Goede V, *et al.* Heterogeneity of angiogenesis and blood vessel maturation in human tumors: implications for antiangiogenic tumor therapies. Cancer Res 2000; 60: 1388-93.

[120] Abramovitch R, Dafni H, Smouha E, Benjamin LE, Neeman M. *In vivo* prediction of vascular susceptibility to vascular susceptibility

endothelial growth factor withdrawal: magnetic resonance imaging of C6 rat glioma in nude mice. Cancer Res 1999; 59: 5012-6.

[121] Gross DJ, Reibstein I, Weiss L, *et al.* The antiangiogenic agent linomide inhibits the growth rate of von Hippel-Lindau paraganglioma xenografts to mice. Clin Cancer Res 1999; 5: 3669-75.

[122] Hsu YY, Chang CN, Jung SM, *et al.* Blood oxygenation level-dependent MRI of cerebral gliomas during breath holding. J Magn Reson Imaging 2004; 19: 160-7.

[123] Kastrup A, Li TQ, Takahashi A, Glover GH, Moseley ME. Functional magnetic resonance imaging of regional cerebral blood oxygenation changes during breath holding. Stroke 1998; 29: 2641-5.

[124] Rostrup E, Larsson HB, Toft PB, *et al.* Functional MRI of CO2 induced increase in cerebral perfusion. NMR Biomed 1994; 7: 29-34.

[125] Kimura H, Braun RD, Ong ET, *et al.* Fluctuations in red cell flux in tumor microvessels can lead to transient hypoxia and reoxygenation in tumor parenchyma. Cancer Res 1996; 56: 5522-8.

[126] Kiani MF, Pries AR, Hsu LL, Sarelius IH, Cokelet GR. Fluctuations in microvascular blood flow parameters caused by hemodynamic mechanisms. Am J Physiol 1994; 266:H1822-H1828.

[127] Cardenas-Navia LI, Yu D, Braun RD, *et al.* Tumor-dependent kinetics of partial pressure of oxygen fluctuations during air and oxygen breathing. Cancer Res 2004; 64: 6010-7.

[128] Chaplin DJ, Olive PL, Durand RE. Intermittent blood flow in a murine tumor: radiobiological effects. Cancer Res 1987; 47: 597-601.

[129] Denekamp J, Dasu A. Inducible repair and the two forms of tumour hypoxia--time for a paradigm shift. Acta Oncol 1999; 38: 903-18.

[130] Kirkpatrick JP, Cardenas-Navia LI, Dewhirst MW. Predicting the effect of temporal variations in PO2 on tumor radiosensitivity. Int J Radiat Oncol Biol Phys 2004; 59: 822-33.

[131] Rofstad EK, Maseide K. Radiobiological and immunohistochemical assessment of hypoxia in human melanoma xenografts: acute and chronic hypoxia in individual tumours. Int J Radiat Biol 1999; 75: 1377-93.

[132] Cairns RA, Kalliomaki T, Hill RP. Acute (cyclic) hypoxia enhances spontaneous metastasis of KHT murine tumors. Cancer Res 2001; 61: 8903-8.

[133] Braun RD, Lanzen JL, Dewhirst MW. Fourier analysis of fluctuations of oxygen tension and blood flow in R3230Ac tumors and muscle in rats. Am J Physiol 1999; 277:H551-H568.

[134] Pigott KH, Hill SA, Chaplin DJ, Saunders MI. Microregional fluctuations in perfusion within human tumours detected using laser Doppler flowmetry. Radiother Oncol 1996; 40: 45-50.

[135] Brurberg KG, Graff BA, Olsen DR, Rofstad EK. Tumor-line specific pO(2) fluctuations in human melanoma xenografts. Int J Radiat Oncol Biol Phys 2004; 58: 403-9.

[136] Baudelet C, Ansiaux R, Jordan BF, *et al.* Physiological noise in murine solid tumours using T2*-weighted gradient-echo imaging: a marker of tumour acute hypoxia? Phys Med Biol 2004; 49: 3389-411.

Received: January 20, 2005 Accepted: February 15, 2005